

## The Possible Role of Allicin in Ameliorating Azithromycin Induced Cardiotoxicity in Adult Male Albino Rat: A Histological and Immunohistochemical Study

Shaimaa Mostafa Kashef and Noha Ramadan. M. Elswaidy

Department of Histology and Cell Biology, Faculty of Medicine, Tanta University, Egypt

### ABSTRACT

**Introduction:** Azithromycin (AZ) is a broad-spectrum macrolide that is incorporated in the treatment of various infectious diseases, and recently enlisted in the protocol of Covid-19 management. Allicin is a classical garlic extraction with cardioprotective, antioxidant, anti-inflammatory, and anti-apoptotic properties.

**Aim of the Work:** To evaluate the cardiotoxic effect of AZ and evaluate the possible protective effect of Allicin against AZ cardiotoxicity using various histological and immunohistochemical techniques.

**Materials and Methods:** Forty adult male albino rats were randomly divided into four main groups: group-I acted as a control group, group-II was given Allicin (20 mg/kg/day) orally for consecutive 14 days, group-III was given AZ (30 mg/kg/day) orally for consecutive 14 days and group-IV was given both AZ and Allicin in the same doses for consecutive 14 days. The cardiac specimens were processed for different histological and immunohistochemical techniques. Morphometrical and statistical studies were also done.

**Results:** Azithromycin induced several myocardial changes in the form of focal areas of destruction of cardiac muscle fibers, darkly stained pyknotic nuclei and cytoplasmic vacuoles. Wavy muscle fibers, widening of the intercellular spaces, mononuclear cellular infiltration, fatty infiltration and hemorrhage were obvious. Dilated and congested blood vessels were also noticed. A significant increase in the mean area percentage of both Masson and  $\alpha$ -SMA immunoreactivity was detected while a significant decrease in the mean area percentage of Bcl-2 was demonstrated. In contrast, most of the histological changes disappeared by Allicin co-treatment except in few localized areas.

**Conclusion:** Azithromycin induced several destructive changes in cardiac muscle fibers. Allicin had a potent ameliorative role in prevention of cardiotoxicity induced by AZ.

**Received:** 18 April 2021, **Accepted:** 24 June 2021

**Key Words:**  $\alpha$ -SMA, allicin, azithromycin, cardiotoxicity, Bcl-2.

**Corresponding Author:** Shaimaa Mostafa Kashef, MD, Department of Histology and Cell Biology, Faculty of Medicine, Tanta University, Egypt, **Tel.:** +20 10 0827 2320, **E-mail:** shaimaa.kashef@med.tanta.edu.eg

**ISSN:** 1110-0559, Vol. 45, No. 3

### INTRODUCTION

Azithromycin (AZ) is a potent antimicrobial antibiotic with well-proved antiviral activity *in vitro* because of its immunomodulating role. It decreases the replication of the virus and prevents its penetration into the host cells, so it has a great role against SARS-CoV-2 activity<sup>[1]</sup>. Moreover, it can manage respiratory infection, skin infection, and soft tissue bacterial infections. It can also be used for long and short-term therapeutic protocols<sup>[2]</sup>. Nowadays, AZ is used in the protocol of treatment of COVID-19 that has affected the world's population since December 2019. It can be used alone or in combination with hydroxychloroquine<sup>[3]</sup>.

Unfortunately, recent studies reported the toxicity of AZ, as it generates a high level of reactive oxygen species (ROS). It is also responsible for many cardiac complications as QTc interval prolongation, ventricular tachycardia, and sudden cardiac arrest especially in the patients with a history of coronary diseases<sup>[4]</sup>.

Nowadays, the world is taking an interest in natural protective extracts that gives new hope for supporting

medicine and minimize the side effects of drugs<sup>[5]</sup>. Nowadays, there are different natural plant-derived cardioprotective agents include: green tea, cocoa, lycopene, resveratrol, grape seed extract, olive oil, and ascorbic acid<sup>[6]</sup>.

Allicin (2-propene-1-sulfinothioic acid S-2-propenyl ester) is a sulfur rich natural extraction of crushed garlic bulb (*Allium Sativum*) and it is the source of the pungent smell of garlic<sup>[7]</sup>. It has distinct criteria as an anti-inflammatory, anti-microbial, cardio-protective, and immunity modulator agent. It may have antiapoptotic properties supporting using it as a treatment of cancer<sup>[8]</sup>.

Considering the outbreak of the new Corona virus in the world, AZ remains the golden treatment that can limit the severity of the disease. Therefore, it was necessary to find a new cheap and available natural plant derived cardioprotective agent to ameliorate AZ-induced cardiotoxicity. For all criteria of Allicin, this work aimed to investigate the ameliorative effect of Allicin against cardiac pathology induced by AZ.

## MATERIALS AND METHODS

### Drugs

AZ is commercially available in a name of Zithromax (250 mg) capsules which is produced by Pfizer Limited Company, USA. Azithromycin (AZ) solution was prepared at a concentration of 6 mg/1ml by dissolving AZ tablet (250 mg) in 41ml distilled water. Allicin powder (code: 2707) was supplied by Mediavet Company for import & export. Kafr El Sheikh, Egypt. Dissolved Allicin solution was prepared at concentration of 4 mg/1ml by dissolving 168 mg Allicin powder in 42 ml saline 0.9.

### Animals

Forty adult male albino rats were employed in this study with an average weight of 180 – 200 grams. They were acclimatized to the laboratory condition for 14 days. The local ethical committee of Tanta University's Faculty of Medicine in Egypt approved all animal work (Approval number: 3429/4/21).

### Study Design

The rats were randomly divided into four main equal groups:

**Group-I (Control group):** consisted of 10 rats that were divided into two equal subgroups:

Subgroup (a): 5 rats received no treatment until the experiment was completed.

Subgroup (b): 5 rats received 1ml of saline 0.9 orally through gastric tube, the diluting vehicle for Allicin powder, for 14 consecutive days.

**Group-II (Allicin group):** 10 rats received Allicin (20 mg/kg/day) orally through gastric tube for consecutive 14 days<sup>[9]</sup>.

**Group-III (AZ group):** 10 rats received AZ (30 mg/kg/day) orally through gastric tube for consecutive 14 days<sup>[10]</sup>.

**Group-IV (AZ+ Allicin group):** 10 rats that were given both AZ (30 mg/kg/day) and Allicin (20 mg/kg/day) for consecutive 14 days.

24 h after the last dose, all animals were received anesthesia in form of intraperitoneal injection of sodium pentobarbital at a dose of 50 mg/kg<sup>[11]</sup>. The heart was excised and cleaned. Specimens from the apex of the left ventricle were excised and prepared for histological and immunohistochemical study.

### Histological Study

Different cardiac sections from each rat in all groups were fixed in 10% formal saline for 24 hours, dehydrated in ascending series of ethyl alcohol then cleared by xylene, and embedded in paraffin. 5  $\mu$ m cardiac sections were cut and exposed to the following stains:

1. Routine hematoxylin and eosin for the general examination of myocardial tissue<sup>[12]</sup>.
2. Masson's trichrome stain for detection of collagen fibers<sup>[13]</sup>.

### Immunohistochemical Staining

Immunohistochemical stains were applied via streptavidin-biotin-peroxidase technique<sup>[14]</sup> using 5- $\mu$ m-thick cardiac sections. These sections were deparaffinized and rehydrated. Then, they were placed in a solution of 3% hydrogen peroxide at room temperature for 10 min then immersed in antigen retrieval solution. Next, the sections incubated with 10% normal goat serum in phosphate buffer solution (PBS) to prevent non-specific protein binding followed by the addition of monoclonal antibody against Bcl-2 (anti-apoptotic protein diluted as 1:200) (Dako, Carpinteria California, USA)<sup>[15]</sup> and  $\alpha$ -SMA primary antibody (1:50) (Abcam, USA)<sup>[16]</sup> to the sections and incubation overnight in a moist chamber at 4°C. Next, drops of streptavidin-peroxidase were added for 20 minutes then rinsed in PBS. Freshly prepared Diaminobenzidine (DAB) solution (as chromogen) was added to the sections for 5-10 minutes followed by washing in PBS for three changes 2 minutes each then counterstained with Mayer hematoxylin. A light microscope (Olympus, Japan) with a built-in camera was used to view and photograph all of the slides in Histology department, Tanta University.

### Morphometric study

The image analysis was carried out with the aid of the program (Image J) (National Institute of Health, Bethesda, Maryland, USA). Ten different non-overlapping randomly selected fields from each slide were quantified for:

1. The mean area percentage of collagen fibers in Masson's trichrome stained sections (X 400)<sup>[17]</sup>.
2. The mean area percentage occupied by brown pixels for Bcl-2 (X 400)<sup>[18]</sup>.
3. The mean area percentage occupied by brown pixels for  $\alpha$ -SMA (X 400)<sup>[19]</sup>.

### Statistical analysis

The collected data were analyzed using one-way analysis of variance (ANOVA), followed by Turkey's test for group comparison. All values were expressed as mean  $\pm$  standard deviation. Differences were regarded as significant if probability *P-value* <0.05 and highly significant if *P-value* <0.001<sup>[20]</sup>.

## RESULTS

Both subgroups of the control group showed no difference in the histological results, so it was referred to both groups as the control group. As regard group-I (control group) & group-II (Allicin group), no statistical difference in the histological or the immunohistochemical results was detected in both groups.

## Histological results

### H&E-stained sections

Histological examination of the myocardium of left ventricle of the control group (group I) showed a normal arrangement of cardiac muscle in form of branched muscle fibers with an acidophilic sarcoplasm and centrally located oval nuclei. Elongated nuclei of interstitial cells as well as connective tissue were seen in between muscle fibers (Figure 1). AZ treated group (group-II) showed atrophy and distortion of cardiac muscles with focal areas of destruction of myocytes (Figures 2,3,4) with mononuclear cellular infiltration (Figures 2,4,5,6). Wavy cardiac fibers were observed (Figures 3,5) while some fibers had darkly stained pyknotic nuclei and cytoplasmic vacuoles (Figure 2). Some cardiac muscle fibers appeared with areas of decreased acidophilia (Figure 4). Additionally, fatty infiltration (Figure 4), a marked widening in the intercellular spaces (Figures 2,5) and hemorrhage (Figures 3,4) were noticed in many sections. Dilated blood vessels with some of their nuclei tend to exfoliate (Figures 5,6). Allicin co-treatment with AZ (group- IV) showed restoration of the normal histological structure of the cardiac muscle except for few cytoplasmic vacuoles (Figures 7,8), and wavy muscle fibers (Figure 8).

### Masson's trichrome results

Cardiac muscle sections of the myocardium of the left ventricle of the control group showed deposition of minimal amounts of blue-stained collagen fibers in between the cardiac muscle fibers and around small blood vessels (Figure 9). Cardiac muscle sections of AZ treated group showed deposition of large amounts of collagen fibers in between cardiac muscle fibers and around dilated blood vessels (Figure 10). Cardiac muscle sections of AZ and Allicin treated group showed a noticeable decrease in the amount of collagen fibers deposited in between cardiac muscle fibers and around blood vessels if compared with AZ treated group (Figure 11).

## Immunohistochemical results

### Immunohistochemistry for Bcl-2

Examination of the Bcl-2 immunostained sections in the control group showed strong positive immunoreactivity for Bcl-2 in most cardiac muscle cells (Figure 12). On contrary, cardiac muscle sections of AZ treated group showed weak cytoplasmic immunoreactivity for Bcl-2 in few cardiac muscle fibers (Figure 13). Cardiac muscle sections of AZ and Allicin treated group showed an apparent increase in the immunoreactivity for Bcl-2 in some cardiac muscles when compared with AZ treated group (Figure 14).

### Immunohistochemistry for $\alpha$ -SMA

Upon our histochemical examination of  $\alpha$ -SMA expression, the control group showed minimal positive immunoreactivity for  $\alpha$ -SMA in the smooth muscle fibers in the blood vessels wall with negative  $\alpha$ -SMA expression in the myocardium (Figure 15). Cardiac muscle sections of AZ treated group showed an increase in the immune expression of  $\alpha$ -SMA in the wall of the blood vessels with the appearance of intensely immune stained elongated cells among the cardiomyocytes (Figure 16). Myocardium sections of AZ and Allicin co-treated group showed an apparent decrease in the immuno-expression of  $\alpha$ -SMA in the wall of blood vessels with a reduction in the number of immune stained elongated cells when compared with AZ treated group (Figure 17).

### Morphometric and statistical analysis

A highly significant increase in the mean area percentage of Masson trichrome stained area was observed in AZ treated group compared to the control group. Also, there was a highly significant decrease of the mean Masson area percentage in AZ and Allicin co-treated group compared to AZ treated group (Table 1, Figure 18).

On the other hand, a highly significant decrement in the mean of Bcl-2 percentage area of AZ treated group compared to the control group. Additionally, a highly significant increase in the mean of Bcl-2 area percentage in AZ and Allicin co-treated group was observed in comparison to AZ treated group (Table 1, Figure 19).

Moreover, a highly significant increase in the mean area percentage of  $\alpha$ -SMA was observed in AZ treated group compared to the control group. Additionally, a highly significant decrease of the mean area percentage of  $\alpha$ -SMA was observed in AZ and Allicin co-treated group compared to AZ treated group (Table 1, Figure 20).

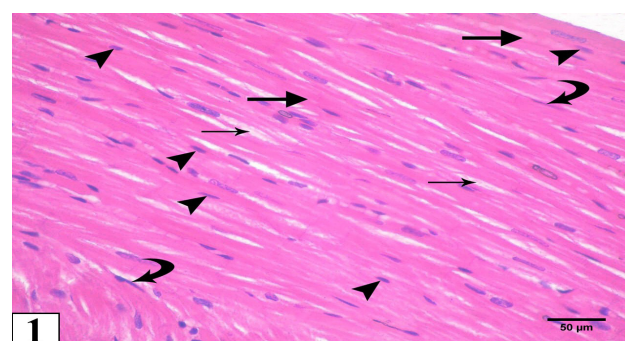


**Fig. 1:** A photomicrograph of the left ventricle of a control rat showing branched cardiac muscle fibers (thick arrow) with an acidophilic sarcoplasm and a centrally located oval nuclei (arrow head). Notice the connective tissue (thin arrow) in between cardiac muscle fibers and elongated nuclei of the interstitial cells (curved arrow) are seen in the interfiber spaces (H.&E., x400).

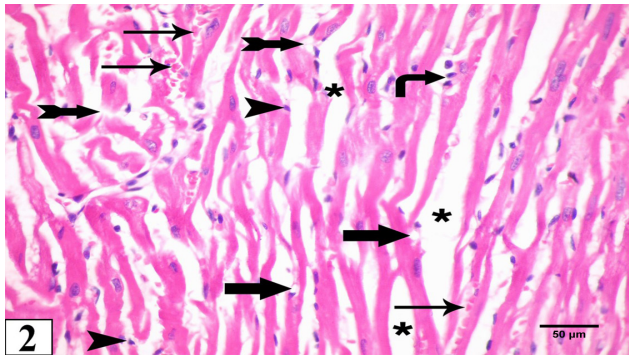


**Fig. 2:** A photomicrograph of the left ventricle of an AZ treated rat showing atrophy and distortion of cardiac muscle with focal areas of destruction of myocytes (notched arrow), darkly stained pyknotic nuclei (arrow head), cytoplasmic vacuoles (thick arrow), and marked widening the tissue space (asterisk). Hemorrhage (thin arrow) and mononuclear cellular infiltration (right angle arrow) is obvious (H.&E., x400).

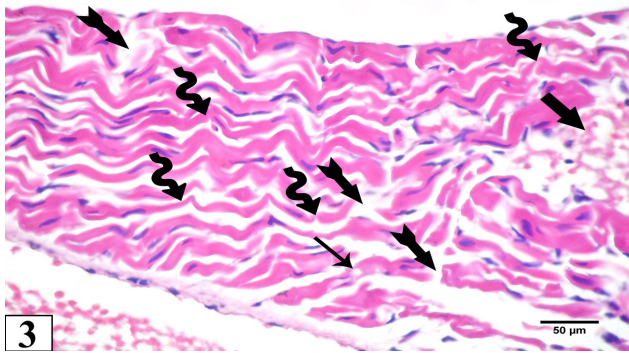


**Fig. 3:** A photomicrograph of the left ventricle of AZ treated rat showing distortion of cardiac muscle with wavy muscle fibers (wavy arrow) and focal areas of destruction of myocytes (notched arrow). Massive hemorrhage (thick arrow) is noticed (H.&E., x400).

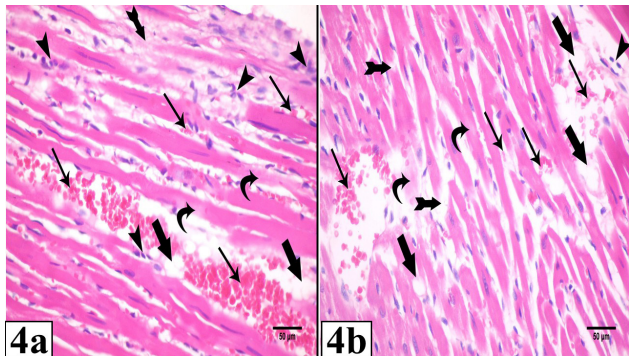


**Fig. 4:** (a) & (b) photomicrographs of the left ventricle of an AZ treated rat showing distortion of cardiac muscle with focal areas of destruction of myocytes (notched arrow) and decreased acidophilia (curved arrow). Hemorrhage (thin arrow), fatty infiltration (thick arrow) and mononuclear cellular infiltration (arrow head) are obvious (H.&E., x400).

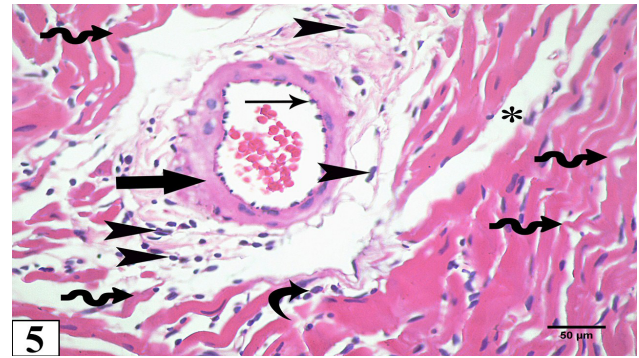


**Fig. 5:** A photomicrograph of the left ventricle of an AZ treated rat showing dilated congested blood vessel with focal thickening in its wall (thick arrow) and its nuclei tend to exfoliate (thin arrow). Wavy muscle fibers (wavy arrow) and marked widening in the tissue space (asterisk) are seen. Notice, perivascular (arrow head) and interfiber mononuclear cellular infiltration (curved arrows) (H.&E., x400).

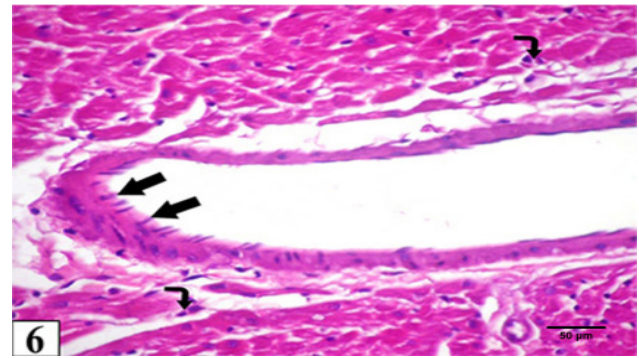


**Fig. 6:** A photomicrograph of the left ventricle of an AZ treated rat showing dilated blood vessel in cardiac muscle. The nuclei of its endothelial cells tend to exfoliate (thick arrows). Notice mononuclear cellular infiltration (right angled arrow)

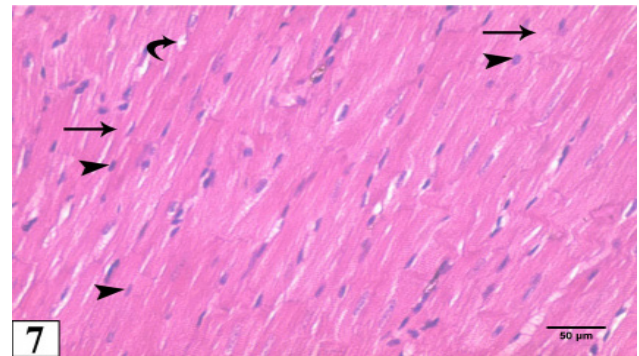


**Fig. 7:** A photomicrograph of the left ventricle of an AZ and Allicin co-treated rat showing normal shaped branched cardiac muscle fibers (arrow) with acidophilic sarcoplasm and centrally located oval nuclei (arrow head). Minimal vacuolization of the cytoplasm (curved arrow) are notice (H.&E., x400).

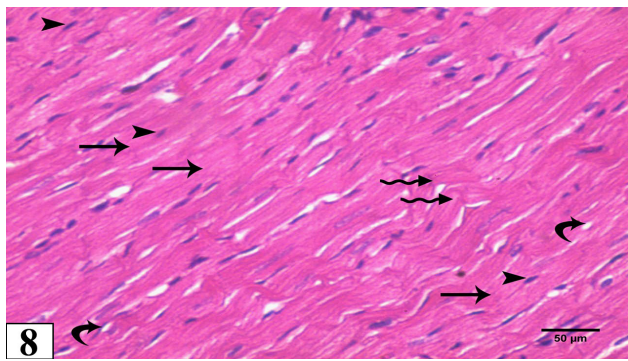


**Fig. 8:** A photomicrograph of left ventricle of an AZ and Allicin co-treated rat showing normal shaped branched cardiac muscle fibers (arrow) with acidophilic sarcoplasm and centrally located oval nuclei (arrow head). Minimal vacuolization of the cytoplasm (curved arrow) and few wavy cardiac fibers (wavy arrow) is notice (H&E., x400).

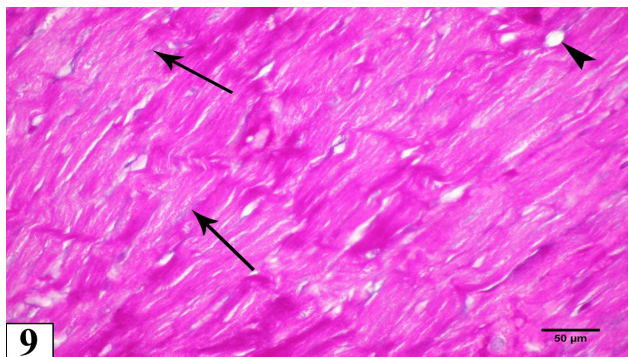


**Fig. 9:** A photomicrograph of the left ventricle of control group showing deposition of minimal amounts of blue stained collagen fibers in between the cardiac muscle fibers (arrow) and around small blood vessel (arrow head). (Masson's trichrome X400).

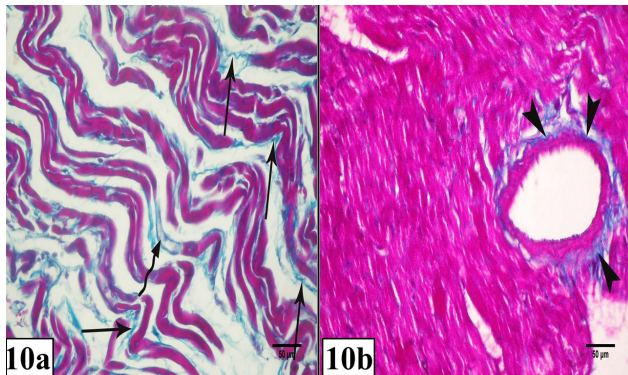


**Fig. 10 (a& b):** photomicrographs of the left ventricle of an AZ treated rat showing deposition of large amounts of blue stained collagen fibers in between cardiac muscle fibers (arrow), at the site of cardiac muscle fibers loss (wavy arrow) and around dilated congested blood vessel (arrow head) (Masson's trichrome X400).

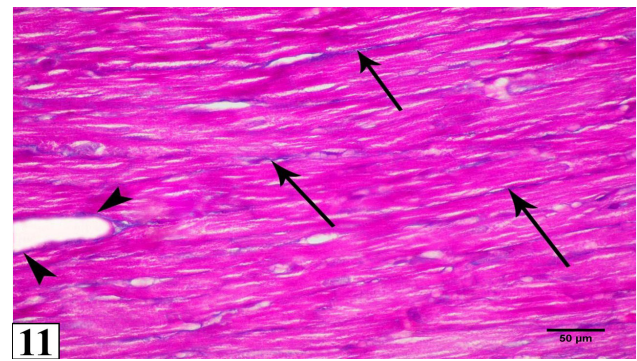


**Fig. 11:** A photomicrograph of the left ventricle of an AZ and Allicin co-treated rat showing deposition of few amounts of blue stained collagen fibers in between cardiac muscle fibers (arrow) and around dilated blood vessel (arrow head) (Masson's trichrome X400).

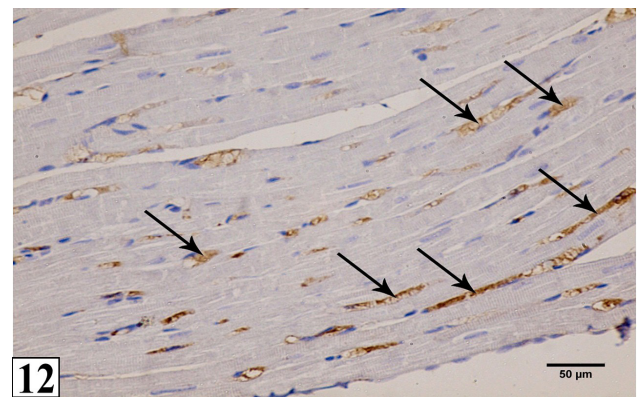


**Fig. 12:** A photomicrograph of the left ventricle of the control group showing strong positive cytoplasmic immunoreactivity for Bcl-2 in most of cardiac muscle cells (arrow) (Bcl-2 immunostaining X400).

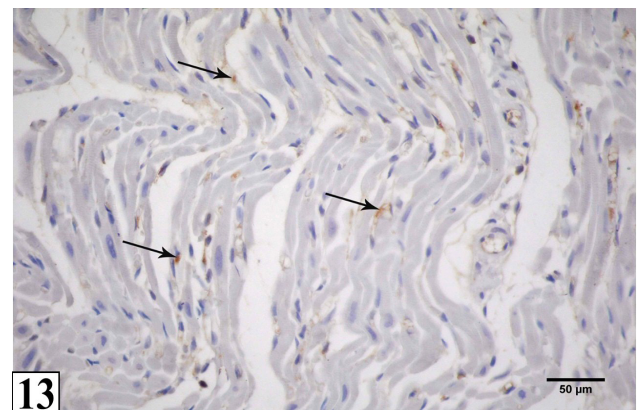


**Fig. 13:** A photomicrograph of the left ventricle of an AZ treated rat showing weak cytoplasmic immunoreactivity for Bcl-2 in few cardiac muscle cells (arrow) (Bcl-2 immunostaining X400).

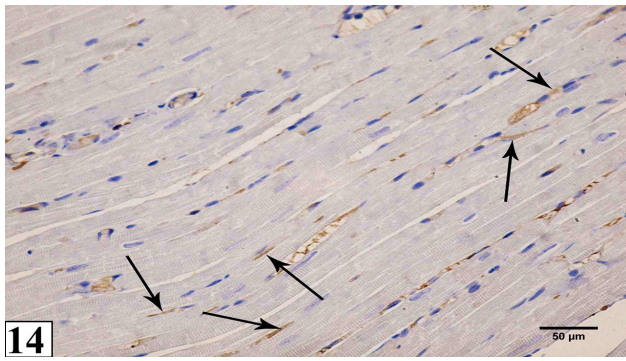


Fig. 14: A photomicrograph of the left ventricle of an AZ and Allixin co-treated rat showing moderate cytoplasmic immunoreactivity for Bcl-2 in some cardiac muscles (arrow) (Bcl-2 immunostaining X400).

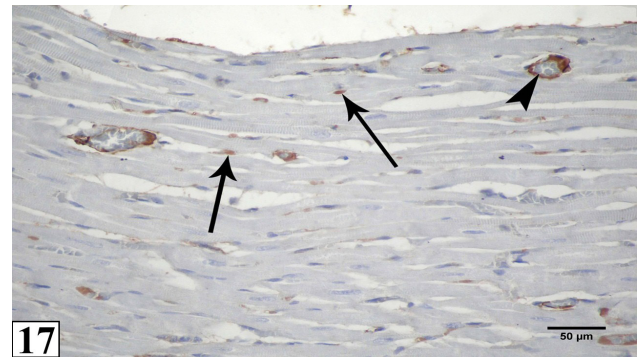


Fig. 17: A photomicrograph of left ventricle of AZ and Allixin co-treated rat showing moderate immunoreactivity of αSMA in the wall of blood vessels (arrow head) with few elongated cells which are moderately immune stained (arrow) in between cardiac muscle cells (α-SMA immunostaining stain X400).

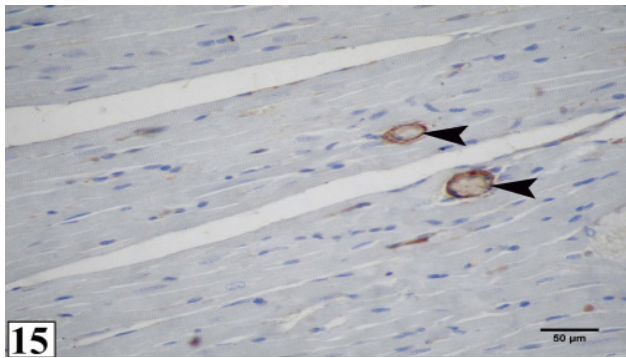


Fig. 15: A photomicrograph of left ventricle of control group showing minimal expression of α-SMA antibody mainly in the wall of the small blood vessels (thin arrow) (α-SMA immunostaining X400).

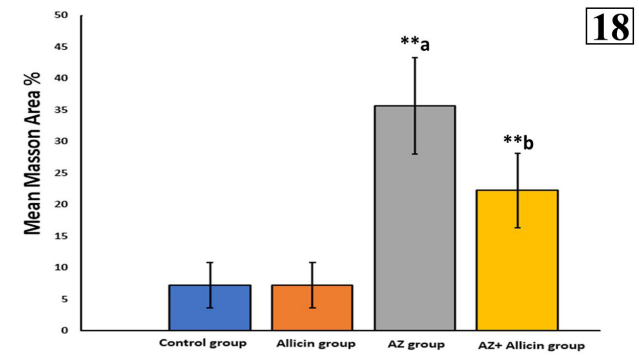


Fig. 18: A histogram showing the mean Masson's trichrome stained area percentage in different groups. \*\* $p < 0.001$ . a versus control group. b versus an AZ group.

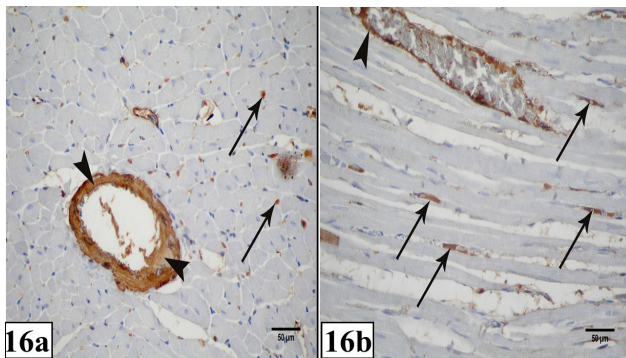


Fig. 16 (a& b): photomicrographs of left ventricle of AZ treated group showing strong immunoreactivity of α-SMA in the wall of blood vessels (arrow head) with appearance of many elongated cells which are strongly immunostained (arrow) in between cardiac muscle fibers (α-SMA immunostaining X400).

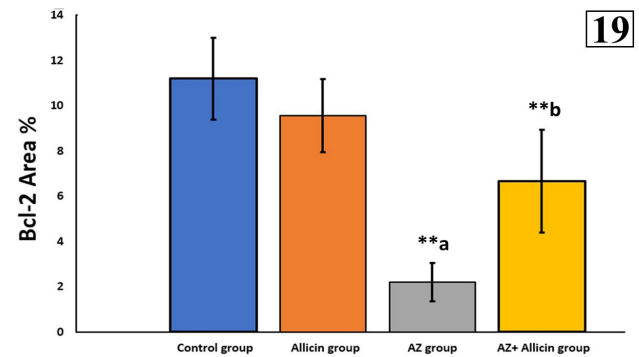


Fig. 19: A histogram showing the mean Bcl-2 stained area percentage in different groups. \*\* $p < 0.001$ . a versus control group. b versus an AZ group.

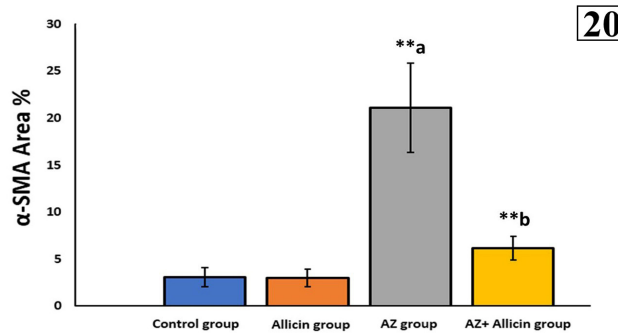


Fig. 20: A histogram showing the mean α-SMA stained area percentage in different groups. \*\* $p < 0.001$ . a versus control group. b versus an AZ group

**Table 1:** Morphometrical and statistical analysis of the means of Masson's trichrome, Bcl-2 and  $\alpha$ -SMA stained areas percentage in different groups

	Control group (Group I)	Allicin group (Group II)	AZ group (Group III)	AZ+ Allicin group (Group IV)
	Mean± SD	Mean± SD	Mean± SD	Mean± SD
Masson's trichrome Area %	7.250±3.565	7.235± 3.570	35.728 ±7.661*	22.259 ± 5.941**
Bcl-2 Area %	11.199 ±1.807	9.570 ±1.626	2.208 ±0.8467*	6.678± 2.270**
$\alpha$ SMA Area %	3.064± 1.025	2.966 ± 0.9383	21.126 ±4.742*	6.198±1.260**

\* Significant versus control.

\*\* Significant versus an AZ group.

## DISCUSSION

AZ is a broad-spectrum macrolide that is widely used to treat various infections especially pneumonia. Moreover, it is one of the drugs enlisted in the protocol of treatment of COVID-19, it may be used as a monotherapy or as a combination with hydroxychloroquine<sup>[21]</sup>. Previous researches documented that AZ induces many ECG changes and clinical presentations as ventricular arrhythmia, cardiac dysfunction, and sudden cardiac collapse in highly susceptible patients<sup>[22]</sup>. Recently, FDA has announced a warning that AZ can participate in potentially fatal arrhythmias. It recommends to prohibit its usage for patients with cardiac diseases<sup>[23]</sup>. So, this creates an urgent need to find a powerful protective agent to minimize its toxicity.

AZ is proved to induce the generation of ROS by suppression of mitochondrial respiration that is followed by DNA oxidative damage. Additionally, it increases the permeability of the mitochondrial membrane that leads to mitochondrial swelling, cytochrome c release in the mitochondria of cardiomyocytes, and induction of apoptosis<sup>[24]</sup>.

Moreover, the damaging effect of AZ occurs because of an interruption in the antioxidant defense system and an increase in the generation of ROS. In this case, the changes in the cardiac performance, ion channels' function, ionic pumps, ion exchange, and inflammatory processes have been related to the oxidative stress induced by AZ in cardiac tissue<sup>[25]</sup>.

On the other hand, cell membrane and intracellular cytoplasmic organelles are damaged by the liberated ROS as they react with phospholipid moieties of the polyunsaturated fatty acids in their plasmalemma<sup>[26]</sup>. Also, it is accompanied by oxidative stress-induced histological changes as loss of cell membranes in the injured cardiac myocytes, marked atrophy of cardiac muscle fibers, and widening of tissue spaces<sup>[27]</sup>.

In our study, AZ treated group showed many changes in the form of distortion of cardiac muscle with focal areas of destruction of myocytes with massive widening in between that coincides with the results of Mansour *et al.*,<sup>[28]</sup>. Additionally, fatty infiltration, and mononuclear cellular infiltration were also detected and were in agreement with the results of Atli *et al.*,<sup>[10]</sup>.

Loss of cardiac myofibers observed in our work may be caused by a reduction in mRNA expression of cardiac-specific proteins, such as troponin I and myosin light chain. Moreover, it may be related to mitochondrial dysfunction that leads to loss of ATP production as well as an imbalance of calcium uptakes that appears in the form of decreased acidophilia (indicating myofibrillar lysis) and prominent sarcoplasmic vacuolation (dilatation of SER of cardiomyocytes)<sup>[29]</sup>.

The nuclei of some cardiomyocytes of AZ treated group were dark stained and pyknotic indicating DNA fragmentation, and apoptosis. This was explained and noticed by Abdel Daim<sup>[9]</sup> in his work on cardiotoxicity induced by doxorubicin.

In the present work, the observed waviness and undulation of muscle fibers were in accordance with Yu *et al.*,<sup>[30]</sup> in his work on myocardial toxicity induced by propofol. It may be explained by the disruption of the connection between the muscle fibrils and the sarcolemma<sup>[31]</sup>. Moreover, other researchers reported that it may appear as a result of forceful systolic tugs by viable fibers adjacent to the non- contractile fibers causing their stretching and folding<sup>[32]</sup>.

The wide spaces in between cardiac muscle fibers and prominent expansion of the interstitium seen in the present study could be attributed to edema in intermuscular spaces and accumulation of mucopolysaccharides in extensive necrotic changes<sup>[33]</sup>. On the other hand, extravasation of RBC's in this study could be attributed to the weakness of the walls of blood vessels caused by inflammation leading to damage of the wall, endothelial cell detachment, vascular leakage, tissue edema, and interstitial hemorrhage<sup>[34]</sup>.

The interstitial mononuclear cellular infiltration seen in Az treated group was explained by Chen *et al.*,<sup>[35]</sup> who stated that free radicals can trigger the inflammatory reactions by cytokines that control leukocytes migration into diseased cardiomyocytes.

Fatty infiltration in between cardiac muscle cells was seen in some areas of the interstitium of Az treated group in our current work that may be explained by fatty degeneration affecting dead cardiomyocytes. This finding was also observed by Khater *et al.*,<sup>[36]</sup> who stated that fibrocytes were transformed into adipocytes at the area of preserved blood flow in the borders of scar tissue.

Many dilated congested blood vessels were observed in our work were observed and interpreted by El-Shitany and El-Desoky<sup>[37]</sup> as a result of an elevated level of serum NO (nitric oxide) by AZ. NO is a powerful vasodilator released by coronary endothelial cells with potent cardioprotective properties minimizing oxidative stress<sup>[38]</sup>. Unfortunately, the elevated level of serum NO induced by AZ indicates myocardial destruction.

On the other side, focal thickening of the vascular wall was also aligned with Jaminon' work<sup>[39]</sup> that explained it as a result of inflammation in the vascular wall and hyperplasia of the smooth muscle of the media. Additionally, in this study, we noticed nuclear protrusions of endothelial cells toward the lumen which was also detected by Pereira *et al.*,<sup>[40]</sup> who stated that this change is a result of oxidative stress.

Bcl-2 proteins are related to the outer mitochondrial membrane and are considered as a guard to the apoptotic reaction. It controls the process of intrinsic apoptosis that begins with the release of cytochrome c and apoptotic factors such as caspase-9 and caspase-3 from the mitochondria<sup>[41,42]</sup>. AZ is reported to induce apoptosis confirmed by analysis of our data that recorded a significant decrease in area percentage of Bcl-2 protein expression in cardiac tissues of Az treated group. Our finding is aligned with the findings of Oda *et al.*,<sup>[43]</sup> on his work on tilmicosin cardiotoxicity.

In our present work. Masson trichrome stained sections of an AZ-groups (group-III) revealed an apparent increase in the amount of collagen fibers deposition between cardiac myofibers and around blood vessels. Moreover, a significant increase in  $\alpha$ -SMA immunostained cells among the cardiomyocytes was observed in this group. These findings were in accordance with the results of Abd El-kader<sup>[44]</sup>. Repair of dead myocardial fibers begins by an uncontrolled multiplication of cardiac fibroblasts that laid an excessive amount of extracellular matrix proteins prompting repairing of the damage and fibrosis. Cardiac fibroblasts form over 90% of the non-myocardial tissues and responsible for the secretion of extracellular proteins and the production of cardioprotective substances<sup>[45]</sup>. They are converted into myofibroblasts in pathological conditions and release excessive fibronectin and collagen fibers leading to myocardial fibrosis, stiffening of the myocardium of the left ventricle, and both systolic and diastolic dysfunction<sup>[46]</sup>. Moreover, these myofibroblasts have the same criteria as fibroblasts and smooth muscle cells so their essence and proliferation in the myocardium can be assessed by  $\alpha$ -SMA<sup>[47]</sup>.

When healthy cardiomyocytes are exposed to free radicals, they start rapidly their defense systems as upregulation of mitochondrial biogenesis and antioxidant agents. Unfortunately, cardiomyocytes are exposed to Az toxicity is more susceptible for damage by them as it contains a lower level of antioxidant enzymes<sup>[48]</sup>.

Alliin is naturally present in garlic and is produced by alliinase enzyme. It is an active sulfur antioxidant that has an oxidative power that can control the oxidative process in the cells. Also, it contributes to the synthesis of macromolecules as DNA, RNA, and protein<sup>[49]</sup>. Hence it was the first reason for our choice for Alliin as a probable protective agent against AZ-induced cardiotoxicity.

To the best of our knowledge, our study is the first to show that Alliin plays a significant role in AZ-induced cardiotoxicity that document the protective role of co-treatment of Alliin with AZ as it improved most of the histological alterations except in few focal areas. Collagen deposition and  $\alpha$ -SMA immunostained cells among the cardiomyocytes decreased while Bcl-2 immunostained cells were increased. Our morphometrical data confirmed our histological data.

In previous researches, Alliin showed a powerful role in myocardial ischemic perfusion injury as it prevents an inflammatory cascade reaction induced by inflammatory factors<sup>[50]</sup>. Also, it has an important role as anti-ischemic, anti-arrhythmic, anti-hyperlipidemic, anti-coagulant, and anti-hypertensive<sup>[51]</sup>. For all previous cardioprotective properties, we supposed that it may a possible role as a protective agent against AZ cardiotoxicity.

Also, Alliin is investigated as anti-microbial, anti-inflammatory, anti-cancer, anti-viral, and antiparasitic drug. It has indicated powerful immunomodulator characters that battle diseases and infections<sup>[52]</sup>. It alleviates myocardium toxicity by clearing ROS as it can reduce circulating ROS and scavenging free radicals in cardiac myocytes by 50% *in vitro* and *in vivo*<sup>[53]</sup>.

Alliin can combine with thiol-possessing enzymes to form a powerful antioxidant. It can be metabolized by cells to produce Alliin derivatives that increase glutathione production. Moreover, it has a role in up-regulating expressions of many genes responsible for decreasing oxidative stress as phase II detoxifying enzymes, cytoprotective enzymes, and enzymes responsible for antioxidant precursors' activation<sup>[54]</sup>.

## CONCLUSION

This work documented the toxic effect of AZ on cardiac muscle causing destructive histopathological changes. Alliin is a powerful protective agent against AZ cardiotoxicity. We recommend further researches in clinical trials for application of Alliin as a promising cardioprotective extract against AZ cardiotoxicity.

## CONFLICT OF INTERESTS

There are no conflicts of interest.

## REFERENCES

1. Mégarbane B and Scherrmann J. Hydroxychloroquine and Azithromycin to Treat Patients With COVID-19: Both Friends and Foes?. *J Clin Pharmacol*. 2020; 60(7):808-14.

2. Hajimirzaei N, Khalili NP, Boroumand B, Safari F, Pourhosseini A, Judi-Chelan R, Tavakoli F. Comparative Study of the Effect of Macrolide Antibiotics Erythromycin, Clarithromycin, and Azithromycin on the ERG1 Gene Expression in H9c2 Cardiomyoblast Cells. *Drug Res (Stuttg)*. 2020;70(8):341-7.
3. Echeverría-Esnal D, Martín-Ontiyuelo C, Navarrete-Rouco, M, De-Antonio Cuscó M, Ferrández O, Horcajada J and Grau S. Azithromycin in the treatment of COVID-19: a review. *Expert Rev Anti Infect Ther*. 2020;1-56.
4. Patel H, DiDomenico R, Suda K, Schumock G, Calip G and Lee T. Risk of cardiac events with azithromycin—A prediction model. *PloS one*. 2020; 15(10): e0240379.
5. Gao W, Wang W, Liu G, Zhang J, Yang J, Deng Z. Allicin attenuated chronic social defeat stress induced depressive-like behaviors through suppression of NLRP3 inflammasome. *Metab Brain Dis*. 2019; 34(1):319-29.
6. Sharifi-Rad J, Rodrigues CF, Sharopov F, Docea AO, Can Karaca A, Sharifi-Rad M, *et al*. Diet, lifestyle and cardiovascular diseases: linking pathophysiology to cardioprotective effects of natural bioactive compounds. *Int J Environ Res Public Health*. 2020;17(7):2326-57.
7. Yang Z, Du J, Zhu J, Rong Y, Chen S, Yu L, Deng X, Zhang X, Sheng H, Yang L and Lu X. Allicin inhibits proliferation by decreasing IL-6 and IFN- $\beta$  in hcmv-infected glioma cells. *Cancer Manag Res*. 2020;12:7305-17.
8. Zhan J, Yan Z, Zhao M, Qi W, Lin J, Lin Z, *et al*. Allicin inhibits osteoblast apoptosis and steroid-induced necrosis of femoral head progression by activating the PI3K/AKT pathway. *Food & Function*. 2020; 11(9):7830-7841
9. Abdel-Daim M, Kilany O, Khalifa H, Ahmed A. Allicin ameliorates doxorubicin-induced cardiotoxicity in rats via suppression of oxidative stress, inflammation and apoptosis. *Cancer Chemother Pharmacol*. 2017;80(4):745-53.
10. Atli O, Ilgin O, Altuntas H and Burukoglu D. Evaluation of azithromycin induced cardiotoxicity in rats, *International Journal of Clinical and Experimental Medicine*. 2015;8(3):3681–90.
11. Ghasi S, Umana I, Ogbonna A, Nwokike M and Ufelle S. Cardioprotective effects of animal grade piperazine citrate on isoproterenol induced myocardial infarction in wistar rats: Biochemical and histopathological evaluation. *African Journal of Pharmacy and Pharmacology*. 2020;14(8):285-93.
12. Gamble, M. 2008. The hematoxylin and eosin. In: JD B, M G, editors. *Theory and Practice of Histological Techniques*. Sixth ed: Churchill Livingstone, Elsevier: Philadelphia. P: 121
13. Liu Z, Naveed M, Baig, M, Mikrani R, Li C, Saeed M, *et al.*, 2021. Therapeutic approach for global myocardial injury using bone marrow-derived mesenchymal stem cells by cardiac support device in rats. *Biomedical Microdevices*. 2021; 23(1): 1-10.
14. Van Noorden S 1990. Principles of immunostaining. In: Filipe, M.I., Lake, B.D. (Eds.) *Histochemistry in Pathology*. Second ed. Churchill Livingstone, Edinburgh. pp. 31-47.
15. Shalaby A and El Shaer, D. Lycopene protects against renal cortical damage induced by nandrolone decanoate in adult male rats. *Annals of Anatomy*. 2019;224: 142-52.
16. Samah K, Aya A, Nafisa A and Reda H. Histological and immunohistochemical study of the effect of alendronate on the submandibular salivary gland of adult male albino rat and the possible protective effect of propolis. *The Medical Journal of Cairo University*. 2018; 86: 3119-32.
17. Ismail Z, Morcos M, EL-Shafei, M and Helmy F. Histological and immunohistochemical study on the possible effect of mangosteen and mesenchymal stem cells on isoproterenol induced myocardial infarction in adult male albino rats. *Egyptian Journal of Histology*. 2019;42(3):651-66.
18. Awad A, Khalil S, Hendam B, Abd El-Aziz R, Metwally, M and Imam T. Protective potency of Astragalus polysaccharides against tilmicosin-induced cardiac injury via targeting oxidative stress and cell apoptosis-encoding pathways in rat. *Environmental Science and Pollution Research*. 2020;27:20861–75.
19. Nasralla M. Possible prophylactic role of quercetin on cisplatin-induced myocardial toxicity in adult male albino rat: histological and immunohistochemical study. *Med. J. Cairo Univ*. 2018;86(1):395-403.
20. Dawson, B. and Trapp, R, (2004). Research questions about relationships among variables (8) in basic & clinical biostatistics. The McGraw-Hill Companies. USA. P: 190-220.
21. Kim Y, Lee S, Yoon J, Kim D, Yu S, Kim J and Kim J. Cardiotoxicity induced by the combination therapy of chloroquine and azithromycin in human embryonic stem cell-derived cardiomyocytes. *BMB reports*. 2020;53(10):545-50.
22. Bakhshaliyev N, Uluganyan M, Enhos A, Karacop E and Ozdemir R. The effect of 5-day course of hydroxychloroquine and azithromycin combination on QT interval in non-ICU COVID19 (+) patients. *Journal of Electrocardiology*. 2020;62: 59-64.

23. Khuroo M. Chloroquine and hydroxychloroquine in coronavirus disease 2019 (COVID-19). Facts, fiction and the hype: a critical appraisal. *Int J Antimicrob Agents*. 2020;56(3):1-13.
24. Salimi A, Eybagi S, Seydi E, Naserzadeh P, Panahi N, Kazerouni N and Pourahmad J. Toxicity of macrolide antibiotics on isolated heart mitochondria: a justification for their cardiotoxic adverse effect. *Xenobiotica* 2016;46(1):82-93.
25. Zhazykbayeva S, Pabel S, Mügge A, Sossalla S, Hamdani N. The molecular mechanisms associated with the physiological responses to inflammation and oxidative stress in cardiovascular diseases. *Biophys Rev*. 2020;12(4):947-68.
26. Meo S, Reed T, Venditti P and Victor V. Role of ROS and RNS sources in physiological and pathological conditions. *oxid med cell longev*. 2016;1245049; 1-45.
27. Bilginoğlu A, Aydın D, Özsoy Ş and Aygün, H. Protective effect of melatonin on adriamycin-induced cardiotoxicity in rats. *Archives of the Turkish Society of Cardiology*. 2014;42(3):265-73.
28. Mansour B, Salem N, Kader G, Abdel-Alrahman G and Mahmoud O. Protective effect of Rosuvastatin on Azithromycin induced cardiotoxicity in a rat model. *Life Sciences*. 2021; 269:119099.
29. Elwan W, Kassab A and Ibrahim M. The possible role of berberine in ameliorating doxorubicin- induced cardiomyopathy in adult male albino rat: a histological and immunohistochemical study. *The Egyptian Journal of Histology*. 2016;39(3):228–40.
30. Yu X, Sun X, Zhao M, Hou Y, Li J, Yu J and Hou Y. Propofol attenuates myocardial ischemia reperfusion injury partly through inhibition of resident cardiac mast cell activation. *Int Immunopharmacol*. 2018; 54:267-74.
31. Grzanka A, Grzanka D and Orlikowska M. (2003): Cytoskeletal reorganization during process of apoptosis induced by cytostatic drugs in K-562 and HL-60 leukemia cell lines, *Biochem Pharmacol*. 2003; 66:1611- 7.
32. Schoen F and Mitchell R (2015): *The heart* (12) in Robbins & Cotran Pathologic Basis of Disease (editors: Kumar V, Abbas A and Aster J). 9<sup>th</sup> Edition. Saunders Elsevier. Philadelphia. USA. P: 523.
33. Savsani H, Shah H, Patel K and Gandhi T. Cardioprotective effect of flavonoids rich fraction of *Premna mucronata* on isoproterenol-induced myocardial infarction in Wistar rats. *Int. J. Phytopharmacol*. 2014;5(2):95-108.
34. Zaghoul S, Abou Elnour R, Abdelfattah M and Ismail D. Comparative histological study on the effect of mesenchymal stem cell and losartan on cardiac injury induced by doxorubicin in male albino rats. *Egyptian Journal of Histology*. 2020;42(4):815-25.
35. Chen L, Deng H, Cui H, Fang J, Zuo Z, Deng J, Li Y, Wang X and Zhao L. Inflammatory responses and inflammation-associated diseases in organs. *Oncotarget*. 2018;9(6):7204-18.
36. Khater N, Selim S, Abd El-Baset S, Abd El Hameed S. Therapeutic effect of mesenchymal stem cells on experimentally induced hypertensive cardiomyopathy in adult albino rats. *Ultrastruct Pathol*. 2017;41(1):36-50.
37. El-Shitany N and El-Desoky K. Protective effects of carvedilol and vitamin C against azithromycin-induced cardiotoxicity in rats via decreasing ROS, IL1- $\beta$ , and TNF- $\alpha$  production and inhibiting NF- $\kappa$ B and caspase-3 expression. *Oxidative Medicine and Cellular Longevity*. 2016;2016:1-14.
38. Banez M, Geluz M, Chandra A, Hamdan T, Biswas O, Bryan N and Von Schwarz E. A systemic review on the antioxidant and anti-inflammatory effects of resveratrol, curcumin, and dietary nitric oxide supplementation on human cardiovascular health. *Nutrition Research*. 2020;78:11-26.
39. Jaminon A, Reesink K, Kroon A, Schurgers L. The Role of vascular smooth muscle cells in arterial remodeling: focus on calcification-related processes. *Int J Mol Sci*. 2019;20(22): 5694.
40. Pereira V, Abidu-Figueiredo M, Pereira-Sampaio M, Chagas M, Costa W and Sampaio F. Sinusoidal constriction and vascular hypertrophy in the diabetes-induced rabbit penis. *Int Braz J Urol*. 2013;39(3):424-31.
41. Khalil S, Abdel-Motal S, Abd-Elsalam M, Abd El-Hameed N and Awad A. Restoring strategy of ethanolic extract of *Moringa oleifera* leaves against tilmicosin-induced cardiac injury in rats: targeting cell apoptosis-mediated pathways. *Gene*. 2020;730144272.
42. Warren C, Wong-Brown W and Bowden N. BCL-2 family isoforms in apoptosis and cancer. *Cell death & disease*. 2019;10(3):1-12.
43. Oda S and Derbalah A. Impact of diclofenac sodium on tilmicosin-induced acute cardiotoxicity in rats (tilmicosin and diclofenac cardiotoxicity). *Cardiovascular Toxicology*. 2020;18(1):63-75.
44. El-kader A. Evaluation of azithromycin induced cardiotoxicity in male albino rats and the possible protective role of nigella sativa oil. *Egyptian Journal of Histology*. 2020;43(2):465-76.
45. Gao Y, Chu M, Hong J, Shang J and Xu D. Hypoxia induces cardiac fibroblast proliferation and phenotypic switch: a role for caveolae and caveolin-1/PTEN mediated pathway. *Journal of Thoracic Disease*. 2014; 6(10):1458-69.
46. Weber K, Sun Y, Bhattacharya S, Ahokas R, Gerling I. Myofibroblast-mediated mechanisms of pathological

- 
- remodelling of the heart. *Nat Rev Cardiol.* 2012;(1):15-26.
47. Gava F, Silva S, Rosa F, Ortiz E, Rodrigues B, Bandarra M, Vasconcelos R and Camacho A. Correlation between systolic function and presence of myofibroblasts in doxorubicin-induced cardiomyopathy. *Ciência Rural.* 2016;46(9): 1642-48.
48. Jiang X, Baucom C and Elliott R. Mitochondrial toxicity of azithromycin results in aerobic glycolysis and DNA damage of human mammary epithelia and fibroblasts. *Antibiotics.* 2019; 8(3): 110-27.
49. Shi X, Zhou X, Chu X, Wang J, Xie B, Ge J, Guo Y, Li X, Yang G. Allicin improves metabolism in high-fat diet-induced obese mice by modulating the gut microbiota. *Nutrients.* 2019;11(12): 2909-13.
50. Liu S, He Y, Shi J, Liu L, Ma H, He L and Guo Y. Allicin attenuates myocardial ischemia reperfusion injury in rats by inhibition of inflammation and oxidative stress. In *Transplantation proceedings.* 2019;51(6): 2060-65.
51. Marón F, Camargo A and Manucha, W. Allicin pharmacology: common molecular mechanisms against neuroinflammation and cardiovascular diseases. *Life sciences.* 2020;249:117513.
52. Fatima S and Dwivedi V. Allicin as an adjunct immunotherapy against tuberculosis. *Journal of Cellular Immunology.* 2020;2(4):178- 82.
53. Oktaviono Y, Amadis M, Al-Farabi M. High dose Allicin with vitamin c improves epe migration from the patient with coronary artery disease. *Pharmacognosy Journal.* 2020;12(2):232-5.
54. Horev-Azaria L, Eliav S, Izigov N, Pri-Chen S, *et al.* Allicin up-regulates cellular glutathione level in vascular endothelial cells. *European journal of nutrition.* 2009; 48(2):67-74.
-

## الملخص العربي

## الدور المحتمل للأليسرين في تحسين السمية القلبية المستحدثة بالإيزيرومايسين في ذكور الجرذان البيض البالغين: دراسة نسيجية وكيمياء نسيج مناعية

شيماء مصطفى كاشف و نهى رمضان محمد السويدي

قسم الهستولوجيا وبيولوجيا الخلية - كلية الطب - جامعة طنطا

**المقدمة:** الإيزيروميسين هو ماكرولايد واسع المجال يدخل في علاج الأمراض المعدية المختلفة، وقد أُدرج مؤخرًا في بروتوكول علاج كوفيد-19. أعلنت إدارة الغذاء والدواء الأمريكية عن تحذير بشأن تسمم القلب بسبب الإيزيروميسين. الأليسرين هو مستخلص تقليدي للثوم مع خصائص وقائية للقلب، ومضاد للأكسدة والالتهابات والإستماتة.

**الهدف من العمل:** يهدف هذا العمل إلى لتقييم تأثير الإيزيروميسين على عضلة القلب لدى الجرذان وتقييم التأثير الوقائي المحتمل للأليسرين ضد السمية القلبية للإيزيروميسين باستخدام تقنيات نسيجية و كيمياء نسيج مناعية مختلفة.

**المواد والطرق:** تم تقسيم 40 من ذكور الجرذان السليمة بشكل عشوائي إلى 4 مجموعات: المجموعة الأولى: و هي المجموعة الضابطة، المجموعة الثانية: المجموعة المعالجة بالأليسرين أعطيت بجرعة 20 مجم / كجم مرة واحدة يوميًا بالفم لمدة 14 يوم، المجموعة الثالثة: أعطيت الإيزيروميسين بجرعة 30 مجم / كجم مرة واحدة يوميًا بالفم لمدة 14 يوم ، المجموعة الرابعة: تلقت كلا من الإيزيروميسين والأليسرين بنفس الجرعات لمدة 14 يوم. تم تجهيز عينات العضلة القلبية للدراسة النسيجية و الكيمياء نسيجية مناعية . تم عمل أيضاً دراسات قياسية و احصائية.

**النتائج:** تسبب الإيزيروميسين في العديد من التغيرات في صورة مناطق مدمرة محدودة في خلايا العضلات القلبية ، نويات داكنة ، وفجوات في السيتوبلازم، وتموج في الألياف العضلية ، واتساع في المسافات البينية ، و تسلل خلوي وحيد النواة وتسلل دهني ونزيف. كما لوحظ تمدد واحتقان الأوعية الدموية. تم الكشف عن زيادة ذو دلالة احصائية في متوسط النسبة المئوية للنشاط المناعي لكل من نسبة الاجزاء المصبوغة بالصبغة الثلاثية و صبغة مضاد  $\alpha$ -SMA. بينما تم الكشف عن انخفاض ذو دلالة احصائية في متوسط نسبة الاجزاء المصبوغة بمضاد Bcl-2. في المقابل، واختفت معظم التغيرات النسيجية عن طريق العلاج المشترك بالأليسرين باستثناء بعض المناطق الموضعية.

**الخلاصة:** تسبب الإيزيروميسين في العديد من التغيرات المدمرة لعضلة القلب. كان للأليسرين دور وقائي فعال في الوقاية من السمية القلبية التي سببها الإيزيروميسين.